

# 白垩纪-古近纪热室地球

杨石岭<sup>1,2\*</sup>, 陈林<sup>1,2</sup>, 纪伟强<sup>1</sup>, 苏涛<sup>3</sup>, 姜仕军<sup>4</sup>, 陈祚伶<sup>1</sup>, 黄晓芳<sup>1</sup>, 郭利成<sup>1</sup>, 王永达<sup>5</sup>, 姜禾禾<sup>1</sup>, 席党鹏<sup>6</sup>, 唐自华<sup>1</sup>, 张师豪<sup>1</sup>, 孙敏敏<sup>1</sup>, 吴福元<sup>1,2</sup>

1. 中国科学院地质与地球物理研究所岩石圈演化与环境演变全国重点实验室, 北京 100029

2. 中国科学院大学地球与行星科学学院, 北京 100049

3. 成都理工大学沉积地质研究院, 成都 610059

4. 海南大学南海海洋资源利用国家重点实验室, 海口 570228

5. 济南大学水利与环境学院, 济南 250022

6. 中国地质大学(北京)地质微生物与环境国家重点实验室, 北京 100083

\* 联系人, E-mail: [yangsl@mail.igcas.ac.cn](mailto:yangsl@mail.igcas.ac.cn)

2025-03-13 收稿, 2025-05-03 修回, 2025-07-07 接受, 2025-07-08 网络版发表

国家重点研发计划(2022YFF0800800)、国家自然科学基金(92479208)和中国科学院地质与地球物理研究所自主部署(IGGCAS-201905)资助

**摘要** 白垩纪-古近纪是距今最近的热室期, 以高温、高大气CO<sub>2</sub>浓度为主要特征。本文梳理了白垩纪-古近纪热室地球的成因、环境特征、生态响应和终结机制等方面的研究进展, 获得以下认识: (1) 根据洋中脊、大陆裂谷、大火成岩省和大陆弧等不同背景岩浆活动的碳释放特征和气候环境记录, 大陆弧岩浆活动很可能是白垩纪-古近纪热室地球形成的主控因素。 (2) 热室背景下发生了多次由碳库扰动引发的极热事件, 如白垩纪大洋缺氧事件(Oceanic Anoxic Events, OAEs)和古新世-始新世极热事件(如Paleocene-Eocene Thermal Maximum, PETM); OAE事件以黑色页岩沉积为特征, 其中OAE1a、OAE1d和OAE2为碳同位素正漂, OAE1b为负漂; PETM等古近纪极热事件则表现为碳同位素负漂, 黑色页岩不发育; 这些差异可能与碳的来源和碳扰动机制不同有关。 (3) 以碳同位素负漂为特征的极热事件发生在长期增温的背景下, 很可能与增温诱发的地表有机碳库热分解有关。 (4) 白垩纪-古近纪热室气候为喜热植物的扩散和物种分化创造了条件, 森林向中、高纬度地区扩张, 植物多样性增加; 海洋中一些微古生物的多样性增加。 总体上, 热室地球的形成和终结与碳的释放和消耗密切相关, 但相关过程的碳释放和消耗通量、剧烈增温对全球降水格局和生态演变的影响尚不明确, 亟待从地球系统角度入手开展多学科交叉研究。

**关键词** 白垩纪-古近纪, 热室地球, 地球深部过程, 碳循环, 极热事件, 环境变化

随着人类碳排放的加剧, 全球温度也不断攀升。为应对气候变化风险, 《巴黎协定》提出将全球增温幅度控制在1.5~2.0°C的目标并倡议全球减排。最近的一些研究认为, 即便实现了《巴黎协定》的目标, 一系列气候系统内部反馈依然有可能使其突破阈值, 从而使地球气候从周期性的冰期-间冰期交替转变为热室状态<sup>[1]</sup>。刚刚过去的2024年是有记录以来最热的一年, 全球平均地表温度比工业化前高出1.55°C, 成为工业革

命以来首个增温超过1.5°C的日历年。如果最近50多年的增温速率持续下去, 至2300年前后地球平均温度将达到20°C, 从而迈入热室的门槛<sup>[2]</sup>, 无论是科学界还是社会公众都担心剧烈增温会引发灾难性的后果。

热室(hothouse)一词最早见于英国作家布里安·阿尔迪斯(Brian Aldiss)的科幻小说*Hothouse*<sup>[3]</sup>, 描述地球停止转动后面向太阳的一侧不断被加热, 热带森林疯狂生长, 少数幸存的人类躲在巨型榕树下生活的场景。

**引用格式:** 杨石岭, 陈林, 纪伟强, 等. 白垩纪-古近纪热室地球. 科学通报

Yang S, Chen L, Ji W, et al. Hothouse Earth during the Cretaceous-Paleogene period: an overview (in Chinese). Chin Sci Bull, doi: [10.1360/CSB-2025-0278](https://doi.org/10.1360/CSB-2025-0278)

地质历史上的热室是指地球平均温度 $>20^{\circ}\text{C}$ 、极地温暖( $5\sim15^{\circ}\text{C}$ )无冰的气候状态<sup>[2]</sup>。白垩纪-古近纪(128~39.4 Ma)是距今最近的热室时期(图1)<sup>[2,4]</sup>, 尤以白垩纪中期(约100~80 Ma)和始新世早期(约56~47 Ma)为代表<sup>[2,5,6]</sup>, 温度和大气CO<sub>2</sub>浓度较高, 热带和亚热带扩张, 高低纬温度梯度显著低于现代, 表生碳库抗扰动能力减弱<sup>[7]</sup>。显然, 研究该热室期有望对未来气候预估提供重要参考。本文梳理了热室气候的成因、环境特征、生态响应和终结机制等方面的研究进展, 并对未来研究进行了展望。

## 1 热室地球的形成

地球90%以上的碳存储在内部圈层, 主要通过不同背景的岩浆活动释放至地球表层系统, 包括洋中脊、大陆裂谷、大火成岩省和大陆弧等(图2)<sup>[8~10]</sup>。洋中脊是地球上最主要的岩浆产生和深部碳释放的场所, 曾被认为是大气CO<sub>2</sub>的主要来源<sup>[11]</sup>。然而, 洋中脊碳释放量难以直接测量, 受洋中脊伸展速率、地幔碳含量和岩浆生成通量等因素影响, 其碳释放通量变化达两个数量级以上<sup>[12]</sup>。有研究认为白垩纪洋中脊扩张速率是现今的1.3~2倍<sup>[13]</sup>, 新生代以来洋中脊扩张速率逐渐降低<sup>[11]</sup>。这与白垩纪热室和温室气候发育、新生代气候长期变冷的特征相一致。但是, 也有研究认为早侏罗世以来(180 Ma)洋中脊扩张速率没有明显变化<sup>[14]</sup>。这些争议主要是由于大洋板块的不断俯冲消减, 洋中脊扩张速率的重建存在很大不确定性<sup>[15]</sup>。此外, 洋中脊碳释放对大气CO<sub>2</sub>浓度的影响也存在争议。其释放的碳主要以CO<sub>2</sub>形式进入海水, 很容易与热的新生洋壳发生反应<sup>[16]</sup>, 或者进入海洋生物有机碳循环<sup>[10]</sup>, 只有洋中脊位于浅水区或暴露于海平面之上才有助于大气CO<sub>2</sub>的增加<sup>[12]</sup>。因此, 洋中脊在长尺度碳循环过程中扮演碳源还是碳汇角色还需要深入研究。

大陆裂谷可以通过深大断裂和岩浆活动释放大陆岩石圈深部存储的碳<sup>[17]</sup>。但是, 地质历史时期裂谷规模重建存在很大不确定性, 同一个裂谷不同部位的碳释放通量也存在显著差异<sup>[18]</sup>。Brune等人<sup>[8]</sup>重建了200 Ma以来全球大陆裂谷长度, 认为两个时间段(160~100 Ma间和~55 Ma以来)裂谷长度很长, 同时大气CO<sub>2</sub>浓度也很高, 从而导致了同期的高温气候。但是, 白垩纪热室期温度很高(图1), 裂谷活动却很弱, 晚新生代(渐新世-中新世)气候变冷但裂谷发育增强。因此, 大陆裂谷对热室地球的形成很可能贡献不大。

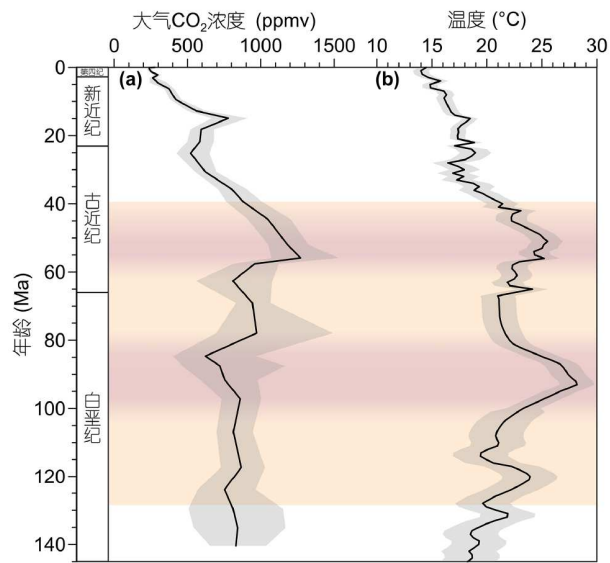


图1 (网络版彩色)白垩纪以来的大气CO<sub>2</sub>浓度和全球温度变化。  
(a) 大气CO<sub>2</sub>浓度<sup>[4]</sup>, 灰色阴影为95%置信限。(b) 全球温度<sup>[2]</sup>, 灰色阴影为均方根误差。水平阴影区指示白垩纪-古近纪热室期

**Figure 1** (Color online) Variations in atmospheric CO<sub>2</sub> concentration and global average temperature since the Cretaceous period. (a) Atmospheric CO<sub>2</sub> concentration<sup>[4]</sup>, with grey shading representing the 95% confidence interval. (b) Global average temperature<sup>[2]</sup>, with grey shading indicating the root mean square error. The horizontal shaded zones highlight the Cretaceous–Paleogene hothouse period

大火成岩省岩浆活动被认为与地质历史上大气CO<sub>2</sub>浓度变化密切相关<sup>[19]</sup>, 其主体部分喷发时间一般小于1 Ma<sup>[20]</sup>。大火成岩省除了通过火山活动直接释放CO<sub>2</sub>, 还可以通过加热富碳沉积地层(如煤和碳酸盐岩)在短期内释放大量含碳气体(CO<sub>2</sub>和CH<sub>4</sub>等), 导致地球快速增温、大洋缺氧和生物灭绝事件的发生<sup>[19]</sup>。大火成岩省主期火山喷发之前, 地壳内部广泛发育岩脉侵入和变质脱碳, 可以解释稍早于大火成岩省峰期的升温事件<sup>[21]</sup>; Black等人<sup>[22]</sup>认为峰期喷发之后, 深部持续的岩浆供给及相关的隐蔽脱气仍然会持续较长的时间, 并据此解释大火成岩省喷发后持续的气候变暖。然而, 大火成岩省主期喷发之前和之后岩浆活动的碳释放量相对于主期喷发更难以确定, 而且只有部分碳释放到大气圈, 气候效应也难以评估<sup>[23]</sup>。此外, 大火成岩省持续时间短, 白垩纪中期和始新世热室期分别持续了20和9 Ma, 很难用大火成岩省一个因素来解释。

大陆弧是影响长期气候变化的重要因素<sup>[24,25]</sup>。大陆弧岩浆中的碳包括俯冲板片、地幔楔和上覆地壳沉积碳酸盐岩等多个来源<sup>[26]</sup>。Lee等人<sup>[24]</sup>发现白垩纪全球

大陆弧总长度(~3.3万km)是现今大陆弧长度的两倍以上(图2(a, c)); 该时期大陆弧上覆地壳中碳酸盐变质脱碳通量比现今高3.7~5.5倍, 足以诱发热室气候。McKenzie等人<sup>[25]</sup>通过汇总和分析全球碎屑锆石年龄, 认为新元古代以来大陆弧长度周期性变化控制了长尺度温室–冰室气候转变和显生宙大气CO<sub>2</sub>浓度波动。全球大陆弧长度重建进一步显示白垩纪大陆弧岩浆活动最强, CO<sub>2</sub>释放通量也最高<sup>[24]</sup>。白垩纪热室期全球大陆弧主要分布于环太平洋和特提斯俯冲带<sup>[24]</sup>。古近纪大陆弧长度明显变短, 太平洋西岸的大陆弧几乎完全消失, 转变为大洋弧(图2(b)), 导致碳释放潜力明显降低。但特提斯造山带东段岩浆大暴发, 岩浆峰期与热室期完全一致, 并且该区域岩浆活动具有高的碳释放潜力, 很可能是古近纪热室期形成的主要控制因素<sup>[27]</sup>。

## 2 热室地球气候环境及生态响应

### 2.1 热室地球气候环境特征

热室地球以高温、高大气CO<sub>2</sub>浓度为主要特征。白垩纪中期几乎是近5亿年来温度最高的时期, 全球平均温度28°C以上<sup>[2,4]</sup>, 热带海表温度可达30°C以上, 中高纬海表温度高于20°C<sup>[28]</sup>。该时期大气CO<sub>2</sub>浓度重建结果差异较大, 介于500~2000 ppmv<sup>[29,30]</sup>, 但Judd等人<sup>[4]</sup>对重建数据采用蒙特卡洛模拟方法获得的大气CO<sub>2</sub>浓度约为800~1000 ppmv。古近纪全球平均温度略低于白垩纪中期, 约25°C以上<sup>[2,4]</sup>, 热带海表温度约30°C以上, 中高纬海表温度高于15°C<sup>[31]</sup>; 大气CO<sub>2</sub>浓度重建结果约为600~3000 ppmv<sup>[30,32]</sup>, 蒙特卡洛模拟方法获得的大气CO<sub>2</sub>浓度约为800~1300 ppmv<sup>[4]</sup>。

从长尺度看, 古近纪大气CO<sub>2</sub>浓度和温度变化较为一致<sup>[33]</sup>, 白垩纪二者的相关性较弱。白垩纪中期温度很高, 但重建的大气CO<sub>2</sub>浓度并不高, 而且整个白垩纪大气CO<sub>2</sub>浓度波动较小<sup>[4]</sup>。这些差异一方面与温度和CO<sub>2</sub>浓度定量重建的准确性有关, 另一方面可能与不同时期地球气候系统内部反馈差异有关, 值得深入研究。

热室气候背景下, 地球气候带分布模式与现今明显不同。气候敏感的沉积岩和矿物指标, 如铝土矿、煤、风成沙丘、蒸发盐、冰碛岩等, 指示白垩纪热室期热带和温带向高纬大幅扩张, 寒带几乎消失, 亚洲地区干旱–半干旱气候占据统治地位(图3)<sup>[9,34]</sup>。根据定量重建结果, 白垩纪热室期北半球中高纬地区湿润, 年降水量可达1200 mm以上<sup>[35]</sup>, 中低纬地区相对干旱。古近

纪热室期气候带分布模式与白垩纪中期类似, 中高纬地区湿润, 年降水量达1000 mm以上<sup>[36]</sup>, 但中低纬干旱带范围较白垩纪中期变小<sup>[34]</sup>。

一些学者<sup>[29]</sup>根据风成沙丘、蒸发岩等记录, 认为白垩纪早期和晚期气候相对偏凉, 哈德来环流向两极扩张, 大气环流强度减弱, 而在白垩纪中期的热室期, 哈德来环流显著收缩<sup>[29]</sup>。这与数值模拟显示的白垩纪热室期副热带高压位置略向赤道移动<sup>[37]</sup>相一致。另一些地质记录和数值模拟结果显示, 白垩纪热室期大气环流很活跃, 强度与现代相似, 且环流位置没有出现向极移动<sup>[38]</sup>。不同模拟结果的差异可能与两个因素有关: (1) 模拟边界条件不一致; (2) 模式参数化方法的差异<sup>[39,40]</sup>。

始新世热室期高分辨率模拟显示, 区域水循环增强<sup>[41]</sup>, 极端降水显著增加<sup>[42]</sup>。多模式集合平均结果显示, 始新世热室期热带辐合带变窄, 中高纬度地区(>30°)和热带地区(<15°)降水增加, 副热带地区(15°~30°)变干<sup>[43]</sup>。不同模式结果对比显示, 高低纬温度梯度控制了副热带地区的干湿状况, 高低纬温度梯度减小, 副热带地区水汽辐散减弱, 干旱程度减轻<sup>[43]</sup>。

### 2.2 热室期的气候敏感度

气候敏感度是指大气CO<sub>2</sub>浓度或其他辐射强迫变化对全球温度的影响, 一般指的是平衡气候敏感度, 即大气CO<sub>2</sub>浓度相对工业革命前翻倍后全球增温的幅度。目前, 针对白垩纪–古近纪热室期的气候敏感度, 已经开展了不少研究<sup>[4,44,45]</sup>, 但无论是定量重建还是数值模拟, 结果差异均较大。白垩纪热室期气候敏感度集中在约2.5~5.5°C<sup>[44,46]</sup>, 始新世热室期气候敏感度集中在约3.6~6.6°C<sup>[45,47]</sup>。有研究认为气候敏感度会随着气候变暖而增加<sup>[33]</sup>, 也有研究认为地球气候敏感度恒定在8°C左右, 对气候背景是温暖还是寒冷没有依赖性<sup>[4]</sup>。造成这些分歧的主要原因是: (1) 热室期地质记录定量重建较少, 且气候指标解译的不确定性较大<sup>[48]</sup>; (2) 热室期古气候模拟分辨率低, 模式中部分物理过程缺失, 且一些模式中的强迫因子在另一些模式中当作反馈使用<sup>[39,44,47,48]</sup>。

### 2.3 热室地球地表碳库扰动

热室地球发生了一系列由碳释放引发的历时数万至数十万年的快速增温事件, 即极热事件, 包括白垩纪的多次大洋缺氧事件(oceanic anoxic events, OAEs)以

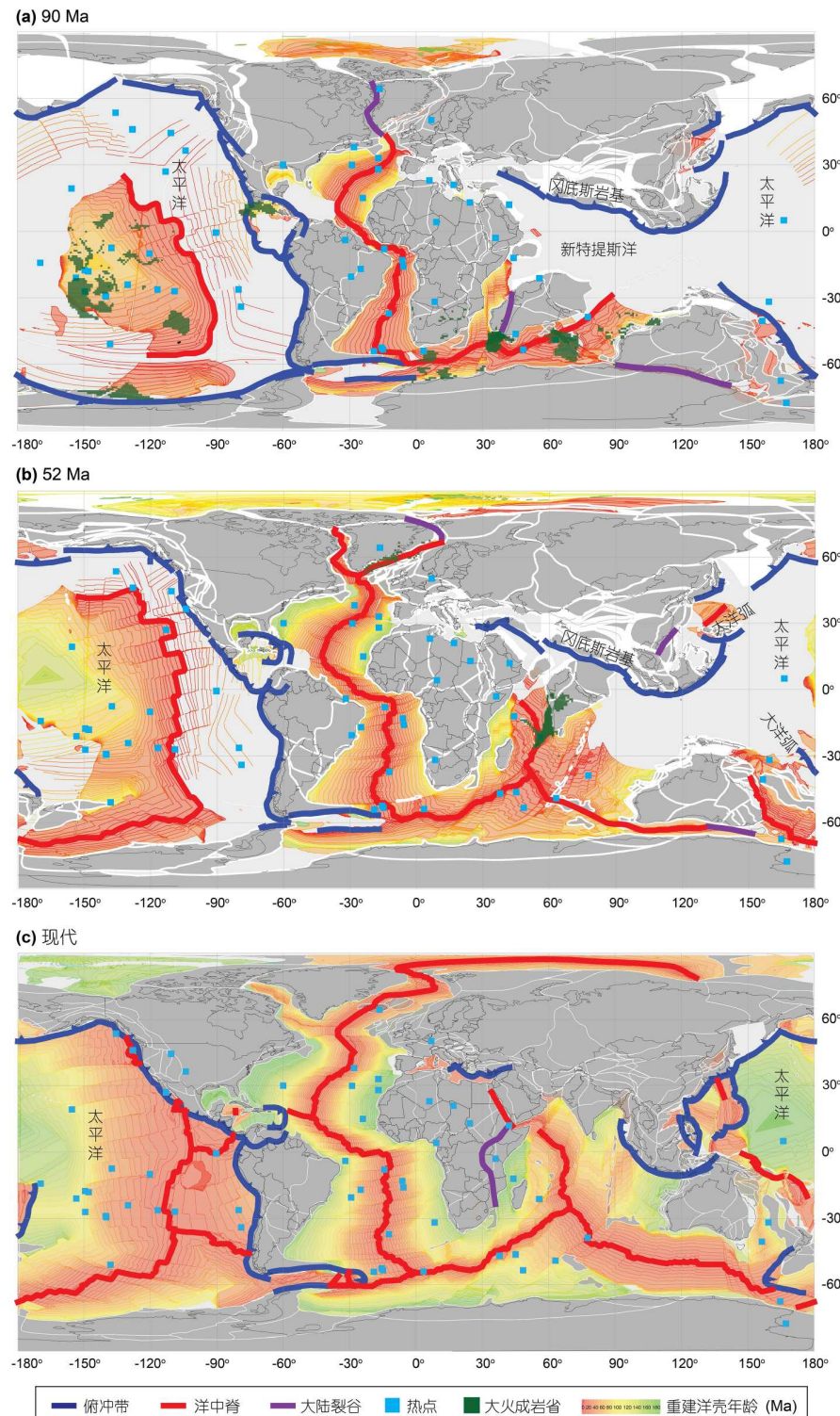


**图 2** 俯冲带、洋中脊、大陆裂谷、热点和大火成岩省分布. (a) 白垩纪热室期(90 Ma). (b) 古近纪热室期(52 Ma). (c) 现代. 大陆裂谷修改自文献[8], 其他构造要素根据文献[9]的板块重建模型获得. (a)和(b)中大火成岩省年龄分别为122~90和62~52 Ma

**Figure 2** Spatial distribution of subduction zones, mid-ocean ridges, continental rifts, hotspots, and large igneous provinces. (a) Cretaceous hothouse period (90 Ma). (b) Paleogene hothouse period (52 Ma). (c) Present-day configuration. The continental rift distribution was modified from Ref. [8], while the positions of other tectonic elements were derived from the plate tectonic reconstruction model developed by Ref. [9]. The large igneous provinces shown in panels (a) and (b) were emplaced during 122–90 and 62–52 Ma, respectively

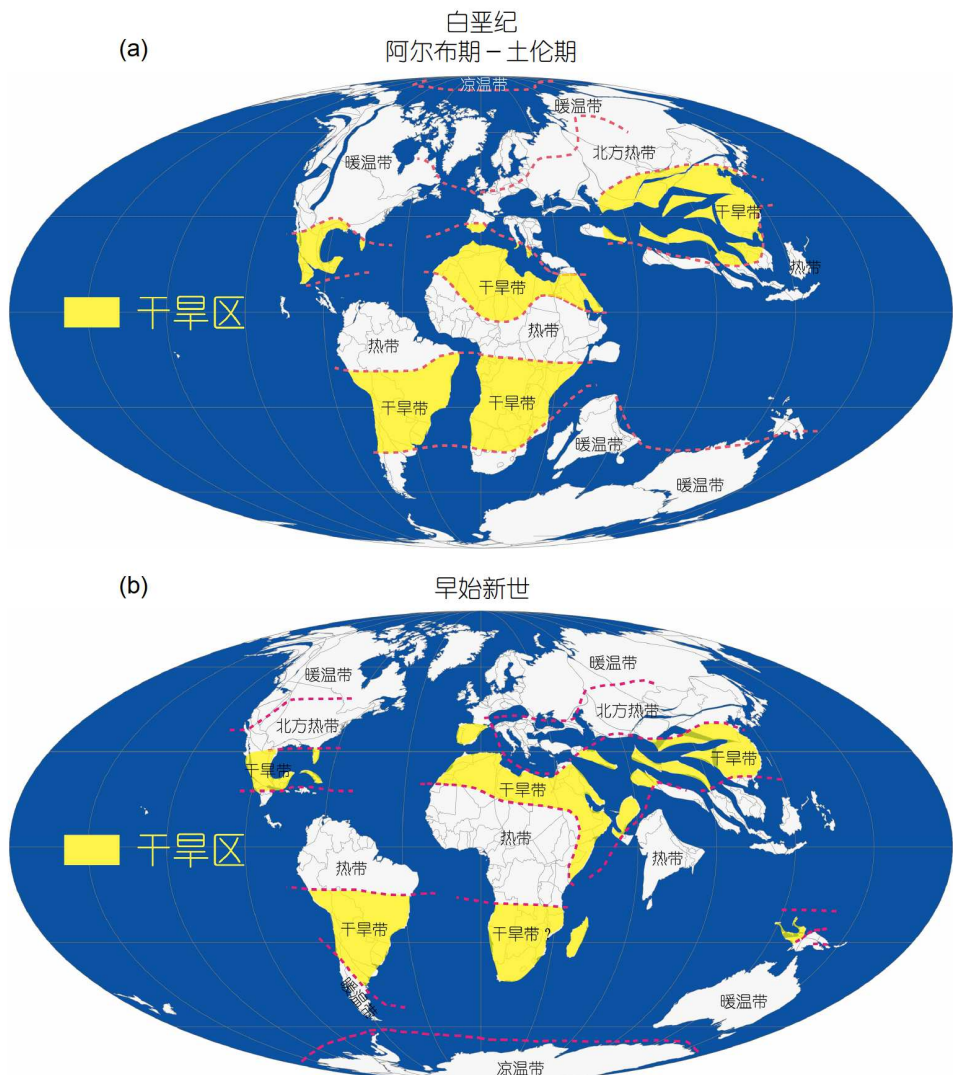


图 3 热室期干旱区分布(修改自文献[34]). (a) 白垩纪阿尔布期–土伦期. (b) 早始新世

Figure 3 Distribution of arid regions during the hothouse periods (modified from Ref. [34]). (a) Albian to Turonian ages of the Cretaceous period. (b) Early Eocene

及古近纪的古新世–始新世极热事件(Paleocene–Eocene Thermal Maximum, PETM)、H1、H2、I1和I2等事件(图4)<sup>[6,49–53]</sup>. 在地质记录上, 白垩纪OAE事件主要表现为黑色页岩沉积, 大部分伴随碳同位素正漂, 少数为碳同位素负漂; 古近纪极热事件则表现为碳同位素负漂, 黑色页岩不发育<sup>[53]</sup>. 这些差异可能与碳的来源和碳扰动机制不同有关.

极热事件期间注入海–气系统的巨量碳主要有两个来源, 地球深部和地球表层有机碳库. 地球深部碳主要来自地幔( $\delta^{13}\text{C}$ :  $\sim -5\text{\textperthousand}$ ), 通过火山活动释放<sup>[54]</sup>. 地球表层有机碳库主要包括泥炭( $\delta^{13}\text{C}$ :  $\sim -25\text{\textperthousand}$ )、土壤有机

物( $\delta^{13}\text{C}$ :  $\sim -25\text{\textperthousand}$ )、冻土( $\delta^{13}\text{C}$ :  $\sim -25\text{\textperthousand}$ )和海底天然气水合物( $\delta^{13}\text{C}$ :  $\sim -60\text{\textperthousand}$ )<sup>[55]</sup>. 这些有机碳库中碳的存储和释放类似电容器的充放电过程, 是地球气候系统的临界要素<sup>[56]</sup>. 当气候系统突破有机碳库分解的阈值时, 会触发有机碳释放–增温这一不可逆的正反馈过程. 地表有机碳库突破临界阈值有两种机制, 一种是火山活动碳释放诱发的初始增温<sup>[57]</sup>, 另一种是天文轨道变动引发的太阳辐射微小变化<sup>[55]</sup>.

白垩纪以碳同位素正漂为特征的典型极热事件是OAE1a( $\sim 120$  Ma)和OAE2( $\sim 94$  Ma), 事件发生初期碳同位素出现负漂移, 随后大幅正漂<sup>[53]</sup>. 这类事件可能主要

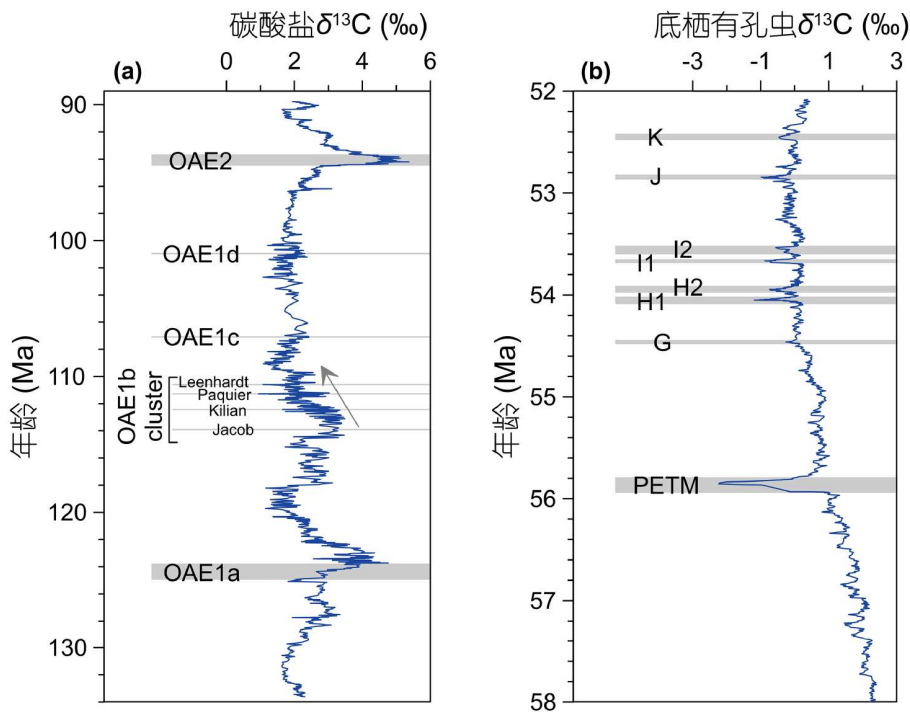


图 4 (网络版彩色)白垩纪和古近纪热室期碳库扰动的碳同位素记录. (a) 白垩纪海洋碳酸盐 $\delta^{13}\text{C}$ 记录<sup>[49,50]</sup>. (b) 古近纪海洋底栖有孔虫 $\delta^{13}\text{C}$ 记录<sup>[6]</sup>.

**Figure 4** (Color online) Carbon isotope records of carbon reservoir perturbations during the Cretaceous and Paleogene hothouse periods. (a) Marine carbonate  $\delta^{13}\text{C}$  record for the Cretaceous<sup>[49,50]</sup>. (b) Deep-sea benthic foraminiferal  $\delta^{13}\text{C}$  record for the Paleogene<sup>[6]</sup>

由海底大火成岩省碳释放引发, 即海底岩浆活动碳释放使海水碳同位素变负, 随着增温和营养元素的大量注入, 海洋生产力提高, 引发海水缺氧和大规模有机质埋藏, 进而引发碳同位素正漂<sup>[58,59]</sup>. OAE2起始阶段的碳同位素负漂只在开阔大洋地区表现明显, 原因可能是局限海盆在事件起始阶段即开始缺氧和有机质快速埋藏<sup>[58]</sup>. OAE1c和OAE1d事件也以碳同位素正漂为特征(也有研究认为OAE1c为碳同位素负漂<sup>[60]</sup>), 但沉积记录相对局限且海洋缺氧程度偏弱, 很可能是区域性事件<sup>[61]</sup>.

白垩纪以碳同位素负漂为特征的典型极热事件是OAE1b, 表现为4层黑色页岩沉积(Jacob、Kilian、Paquier和Leenhardt)<sup>[50,62]</sup>. OAE1b的碳同位素负漂是全球性的, 而黑色页岩只发育在部分海域, 表明海洋缺氧是区域性的<sup>[63]</sup>; 该事件沉积地层中出现 $^{187}\text{Os}/^{188}\text{Os}$ 降低的现象<sup>[64]</sup>, 指示地幔来源非放射性成因的Os增加, 被归因于海底大火成岩省活动<sup>[64,65]</sup>. 但是, 最近的湖泊和海洋记录中发现OAE1b的部分碳同位素负漂事件滞后于Hg的富集<sup>[65,66]</sup>, 而且OAE1b的4个负漂事件发生在OAE1b早期至晚期碳同位素长期负漂(图4(a))、温度逐渐升高

的背景下<sup>[50,67]</sup>, 表明火山活动引发的前期增温导致地表有机碳库碳释放很可能是触发OAE1b事件的机制.

古近纪热室期的系列极热事件均表现为显著的碳同位素负漂(图4(b)). 一些研究认为, 这些极热事件与天文因素有关, 主要依据是极热事件与地球轨道偏心率最大值在时间上相吻合<sup>[68]</sup>, 但亦有研究认为二者在时间上并不一致<sup>[51]</sup>. 因此, 轨道因素对极热事件的影响尚存有争议. 富含 $^{12}\text{C}$ 的彗星撞击<sup>[69]</sup>和构造抬升引发陆缘海沉积有机碳分解<sup>[70]</sup>虽被提出作为极热事件触发机制, 但撞击事件的随机性和百万年尺度的构造过程难以合理解释早始新世的多次短暂极热事件. 另一方面, PETM事件发生之前沉积记录出现明显的Hg富集<sup>[57]</sup>和增温<sup>[71]</sup>, 意味着火山活动触发了前期增温并诱发地表有机碳库的碳释放.

由此看来, 针对热室地球地表碳库扰动诱因的争议, 仍需要从三个方面深入研究: (1) 开展高精度绝对定年工作, 获取极热事件与天文轨道的准确关系; (2) 系统开展Hg含量及Hg和Os同位素分析, 厘清深部过程在极热事件发生时期的作用; (3) 围绕极热事件开展高分辨率碳同位素分析和温度重建, 揭示两者之间

的耦合关系。

相比较而言，白垩纪OAE事件碳同位素变化的解释机制比古近纪极热事件复杂。理解这一问题需要注意的是：白垩纪OAE事件最核心的判别标准是大洋缺氧导致的黑色页岩沉积<sup>[72]</sup>，碳同位素特征比较复杂，而古近纪极热事件从研究伊始就是基于海洋沉积的氧、碳同位素变化来研究温度和碳库扰动的。因此，二者的比较需要在同一个逻辑框架下开展。

极热事件期间碳库扰动引发了显著的气候环境变化。巨量CO<sub>2</sub>释放引发的海洋酸化使部分海洋生物灭绝<sup>[73]</sup>，陆地上气候带大幅移动并导致动植物的迁移和快速演化，但未引发生物灭绝<sup>[74,75]</sup>。极热事件期间水循环明显加快，但降雨变化却存在显著时空差异<sup>[76]</sup>。OAE1a时期，中低纬地区的南欧<sup>[77]</sup>和中国东部<sup>[78,79]</sup>发生了显著干旱化，湖泊盐度增加、缺氧<sup>[78,79]</sup>。OAE1b时段中国东部气候温暖湿润，化学风化增强，湖泊有机质富集<sup>[80]</sup>。OAE2时期南半球高纬澳大利亚地区气候温暖湿润，地表径流增强<sup>[81]</sup>，北半球中纬法国一带气候整体比较湿润<sup>[75]</sup>。总体上，白垩纪大洋缺氧事件期间陆地气候环境记录还比较稀少。

PETM时期高纬地区降雨量整体增加<sup>[82,83]</sup>，中低纬地区降雨变化则相对复杂。该时期，东亚地区降雨量整体增加，且纬度越高降雨增幅越大<sup>[84]</sup>，欧洲地区则表现为极端降雨事件明显增多<sup>[85]</sup>；北美地区在事件前期变干，后期干湿交替<sup>[86]</sup>。全球野火活动在PETM时期与降雨的时空变化密切相关<sup>[87]</sup>，相对湿润的地区和时段野火活动较弱，相对干旱的地区和时段野火活动较强。

## 2.4 热室地球生态响应

有研究认为，全球增温将导致大量物种灭绝、生物多样性丧失，危及生态系统安全<sup>[88]</sup>。但地质记录显示，白垩纪–古近纪热室期被子植物显著分化并在陆地生态系统中占据主导地位，逐渐奠定了现今的植物多样性面貌和空间分布格局<sup>[89]</sup>。

热室气候及海陆格局变化极大促进了洲际植物区系成分的交流。龙脑香科是现今亚洲热带雨林的代表类群，该类群在白垩纪热室时期起源于非洲，白垩纪末期传播到印度次大陆，随着印度板块与欧亚大陆的拼合，在始新世热室期扩散到东南亚<sup>[90]</sup>，说明现代亚洲热带雨林丰富的植物多样性很可能是热室气候下本土物种和大量外来物种交融的结果。棕榈科主要分布于热带地区，最早的棕榈科化石见于法国晚白垩世地层<sup>[91]</sup>，

随后迅速在全球中低纬地区广泛分布<sup>[92]</sup>，早始新世甚至出现在北极地区的新西伯利亚群岛<sup>[93]</sup>。适应炎热气候的狭叶梅属(*Palibinia*)可能在古新世时期起源于我国东南部，始新世中晚期扩散到我国西北以及北美和欧洲<sup>[94]</sup>。因此，白垩纪–古近纪热室气候为全球众多喜热植物类群的扩散和物种分化创造了条件。

热室期全球森林向中、高纬度地区扩张，两极地区发育温带森林，群落结构发生显著改变。白垩纪–古近纪界限之后，中美洲植物的新物种形成速率和多样性大幅增加<sup>[95]</sup>，林冠结构更为复杂，形成丰富的植物生长习性，出现新热带的现代雨林基本特征<sup>[89]</sup>。PETM极热期北美大陆的众多植物类群向北迁移650~1500 km<sup>[96]</sup>，始新世热室期新热带的植物多样性达到峰值<sup>[95]</sup>，说明热室气候有利于植被扩张和物种多样性增加。热室气候还深刻影响了生态系统的结构：随着白垩纪被子植物的逐渐繁盛，被子植物的虫媒传粉方式出现<sup>[97]</sup>；白垩纪–古近纪灭绝事件对植食性昆虫的取食行为产生干扰，使得植食性昆虫多样性在短时期内显著下降<sup>[98]</sup>；但是在白垩纪–古近纪灭绝事件之后，伴随着以被子植物为绝对优势的现代热带雨林出现，以及裸子植物为主的针叶林消退，访花昆虫开始大量分化并繁盛至今<sup>[97]</sup>。此外，PETM时期植食性昆虫的取食频率和取食形态多样性均有明显上升<sup>[99]</sup>，可能意味着植食性昆虫种类的增加<sup>[100]</sup>。

热室气候对一些微古生物的多样性有重要影响(图5)<sup>[101,102]</sup>。比如，浮游有孔虫(图5(b))在白垩纪中期非常繁盛，白垩纪末期发生了显著的灭绝，之后逐渐复苏，并在始新世中期多样性达到峰值；沟鞭藻(图5(c))和钙质超微生物(图5(d))的多样性整体上在白垩纪中、晚期较高，白垩纪末至古近纪初减少，始新世早期又迅速增加。硅藻(图5(e))和放射虫(图5(f))的多样性对热室气候的响应不显著，但随着晚新生代全球变冷，多样性逐渐增加。总体而言，温暖水体环境有利于钙质类和部分有机质类微体生物，而温凉甚至较冷的水体环境有利于硅质类微体生物(如放射虫和硅藻)。

总之，白垩纪和古近纪热室期都是高温、高大气CO<sub>2</sub>浓度时期，但其环境要素、气候敏感度、地表碳库扰动过程及机制不尽相同(表1)。从已有研究结果看，这两个热室期的环境状况都有利于生物多样性的增加。

## 3 热室地球的终结

热室气候维持数百万年至上千万年后，随大气CO<sub>2</sub>

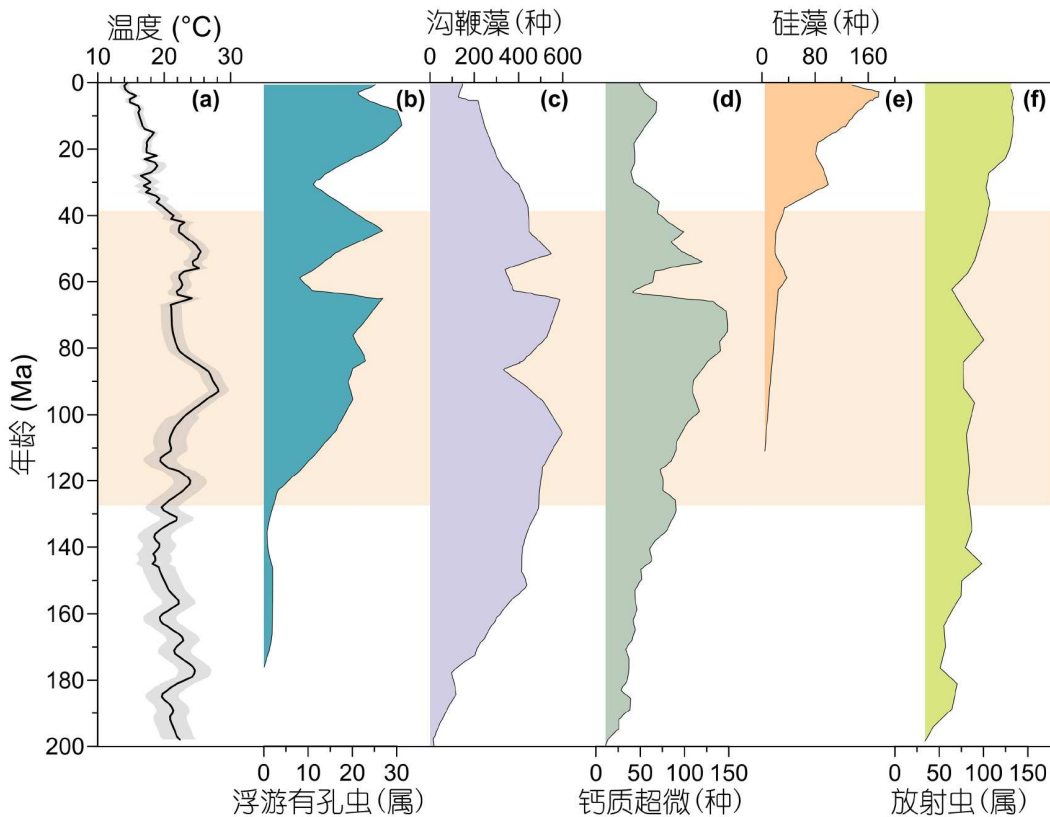


**图 5** (网络版彩色)两亿年来全球温度变化与海洋微体生物多样性演化. (a) 全球温度<sup>[2]</sup>, 阴影为均方根误差. 浮游有孔虫(b)、沟鞭藻(c)、钙质超微(d)和海洋硅藻(e)多样性曲线, 据文献[101]修改. 放射虫(f)多样性曲线, 据文献[102]修改. 水平阴影区指示白垩纪-古近纪热室期

**Figure 5** (Color online) Evolution of global temperature and marine microfossil diversity over the past 200 million years. (a) Global average temperature<sup>[2]</sup>, with grey shading indicating the root mean square error. Diversity trends are shown for (b) planktic foraminifera genera, (c) dinoflagellate cyst species, (d) nannofossil species, and (e) marine diatom species, adapted from Ref. [101], and (f) radiolarian genera, adapted from Ref. [102]. The shaded zone highlights the Cretaceous–Paleogene hothouse period

**表 1** 白垩纪和古近纪热室期气候、环境和生态响应对比

**Table 1** Comparison of climatic, environmental, and ecological responses between the Cretaceous and Paleogene hothouse periods

环境要素/特征		白垩纪热室期	古近纪热室期
温度	全球平均 <sup>[2,4]</sup>	>28°C	>25°C
	海表	>30°C (低纬) <sup>[28]</sup> >20°C (中高纬) <sup>[28]</sup>	>30°C (低纬) <sup>[31]</sup> >15°C (中高纬) <sup>[31]</sup>
	大气CO <sub>2</sub> 浓度	500~2000 ppmv (指标) <sup>[29,30]</sup> 800~1000 ppmv (集成) <sup>[4]</sup>	600~3000 ppmv (指标) <sup>[30,32]</sup> 800~1300 ppmv (集成) <sup>[4]</sup>
气候敏感度		约2.5~5.5°C <sup>[44,46]</sup>	约3.6~6.6°C <sup>[45,47]</sup>
地表碳库 扰动	碳同位素正漂移	OAЕ1a、OAЕ1c、OAЕ1d、OAЕ2 <sup>[49,50]</sup>	-
	碳同位素负漂移	OAЕ1b (Jacob, Kilian, Paquier, Leenhardt) <sup>[49,50]</sup>	PETM、G、H1、H2、I1、I2、J、K等 <sup>[6,51]</sup>
生态响应	植物	被子植物快速扩散、分化 <sup>[90,92]</sup>	现代热带雨林出现 <sup>[89]</sup>
	昆虫	被子植物的虫媒传粉方式出现 <sup>[97]</sup>	访花昆虫分化繁盛 <sup>[97]</sup>
	海洋微古生物 多样性	浮游有孔虫、沟鞭藻、钙质超微生物繁盛; 硅藻和放射虫多样性无显著变化 <sup>[101,102]</sup>	浮游有孔虫、沟鞭藻、钙质超微生物繁盛; 硅藻和放射虫多样性无显著变化 <sup>[101,102]</sup>

的逐渐消耗而终结. 在此过程中, 硅酸盐风化<sup>[103]</sup>和有机碳埋藏<sup>[104]</sup>起了关键作用. 白垩纪-古近纪火山活动

活跃, 全球温度高, 水循环增强<sup>[105]</sup>, 风化也随之增强<sup>[106,107]</sup>. 有研究<sup>[108]</sup>认为坎潘期(83.6~72.1 Ma)中晚期

海洋黏土矿物显著增加，说明陆地化学风化增强是导致大气CO<sub>2</sub>下降和全球降温的重要因素。

白垩纪–古近纪我国东部和南部季风盛行<sup>[109]</sup>，湖泊、河口和陆架有机质埋藏活跃<sup>[110,111]</sup>。热室地球一些地区高温高湿的气候不仅有利于陆地植被的发育，而且还随着大陆风化产物的搬运给海洋和湖泊带来大量的营养物质<sup>[112]</sup>，导致水体初级生产力大幅增加并缺氧<sup>[113]</sup>，缺氧环境下沉积物中的磷释放到水体中<sup>[114]</sup>，导致生物生产力进一步增加，最终形成广泛的黑色页岩沉积<sup>[115]</sup>。此外，白垩纪–古近纪沙漠广泛分布(图3)<sup>[34]</sup>。在西风作用下，这些干旱区会向海洋输送大量粉尘，粉尘的“铁施肥效应”<sup>[116]</sup>有利于浮游植物的生长，从而吸收大量CO<sub>2</sub>并引发全球降温。但这方面研究还比较薄弱，值得关注。

白垩纪–古近纪碳消耗的定量研究主要依赖于地球化学模型，已有研究认为白垩纪热室期大陆风化的碳消耗量为40.7 MtC/a<sup>[117]</sup>，有机碳埋藏的碳消耗量为34.5~64.1 MtC/a<sup>[117,118]</sup>；古近纪热室期大陆风化的碳消耗量为33.3~146.2 MtC/a<sup>[103,117]</sup>，有机碳埋藏的碳消耗量为22.3~132.8 MtC/a<sup>[117,118]</sup>。已开展的地质记录集成工作主要聚焦在OAE2事件期间的有机碳埋藏速率<sup>[111,119]</sup>。总体上白垩纪–古近纪碳消耗的定量研究较为薄弱，不同模型的估算结果差异很大，需要地质大数据综合集成来交叉验证。

## 4 问题和展望

大陆弧岩浆作用具有明显的暴发–间歇特点，不同阶段对碳循环贡献完全相反：早期岩浆活动频繁，为碳源；晚期岩浆活动减弱，剥蚀风化作用增强，为碳汇<sup>[120]</sup>。

大陆弧早期岩浆–变质作用放碳和后期剥蚀风化吸碳很可能是热室地球形成和终结的主要因素，但相关的碳释放和消耗通量尚不明确，需要通过地质记录与模型相互校验、大数据综合分析等的集成研究，厘定全球和区域碳释放和碳消耗通量。

热室期的温度和大气CO<sub>2</sub>浓度是理解热室气候维持机制的最为关键的环境要素，目前二者的重建结果并不完全吻合。围绕这个问题，既要加强环境要素定量重建的可靠性，也要加强气候敏感度的研究。增温过程中，水循环的时空演变与大气环流格局的改变密切相关，但目前相关方面的研究较少。此外，热室期区域降水的定量重建也十分缺乏，年代际、年际甚至季节性的高分辨率研究也需要积极探索。通过地质记录和数值模拟重建温度、降水以及大气环流格局，揭示快速增温背景下水循环变化的动力学机理，是研究热室地球的核心任务。

以碳同位素负漂为特征的极热事件发生在长期增温的背景下，表明地表有机碳库对全球增温比较敏感。OAE1b和PETM以及始新世极热事件很可能都由地表有机碳库扰动引发，亟待开展碳释放量及其环境效应的对比研究。这有助于深入理解地球系统内反馈机制，并为评估未来碳排放的环境效应提供科学支撑。

热室气候对陆地生态系统的物种组分、植被面貌、群落结构等产生了重大影响，但是目前陆地生态系统具体如何响应热室气候尚不明确，亟需通过高分辨率植被演化序列重建和高精度植被模拟交叉验证，并开展热室时期陆地生态系统与环境协同演化的集成研究，进而解析陆地生态系统对热室气候的响应与适应过程及其机制。

**致谢** 感谢中国科学院地质与地球物理研究所赵亮研究员在组稿中给予的大力帮助，美国德克萨斯州大学阿灵顿分校Christopher R. Scotese教授提供部分资料，4位审稿人提出宝贵建议。

## 参考文献

- 1 Steffen W, Rockström J, Richardson K, et al. Trajectories of the Earth System in the Anthropocene. *Proc Natl Acad Sci USA*, 2018, 115: 8252–8259
- 2 Scotese C R, Song H, Mills B J W, et al. Phanerozoic paleotemperatures: the Earth’s changing climate during the last 540 million years. *Earth-Sci Rev*, 2021, 215: 103503
- 3 Aldiss B. Hothouse. London: Faber and Faber, 1962. 1–253
- 4 Judd E J, Tierney J E, Lunt D J, et al. A 485-million-year history of Earth’s surface temperature. *Science*, 2024, 385: eadk3705
- 5 Zachos J C, Dickens G R, Zeebe R E. An early Cenozoic perspective on greenhouse warming and carbon-cycle dynamics. *Nature*, 2008, 451: 279–283

- 6 Westerhold T, Marwan N, Drury A J, et al. An astronomically dated record of Earth's climate and its predictability over the last 66 million years. *Science*, 2020, 369: 1383–1387
- 7 Armstrong McKay D I, Lenton T M. Reduced carbon cycle resilience across the Palaeocene–Eocene Thermal Maximum. *Clim Past*, 2018, 14: 1515–1527
- 8 Brune S, Williams S E, Müller R D. Potential links between continental rifting, CO<sub>2</sub> degassing and climate change through time. *Nat Geosci*, 2017, 10: 941–946
- 9 Scotese C R, Vérard C, Burgener L, et al. The Cretaceous world: plate tectonics, palaeogeography and palaeoclimate. In: Hart M B, Batenburg S J, Huber B T, et al., eds. Cretaceous Project 200 Volume 1: The Cretaceous World. Colombia: Geological Society, London, Special Publications, 2024. 544
- 10 Lee C T A, Jiang H, Dasgupta R, et al. A framework for understanding whole-earth carbon cycling. In: Orcutt B N, Daniel I, Dasgupta R, eds. Deep Carbon: Past to Present. Cambridge: Cambridge University Press, 2019. 313–357
- 11 Berner R A, Lasaga A C, Garrels R M. The carbonate-silicate geochemical cycle and its effect on atmospheric carbon dioxide over the past 100 million years. *Am J Sci*, 1983, 283: 641–683
- 12 Le Voyer M, Hauri E H, Cottrell E, et al. Carbon fluxes and primary magma CO<sub>2</sub> contents along the global mid-ocean ridge system. *Geochem Geophys Geosyst*, 2019, 20: 1387–1424
- 13 Becker T W, Conrad C P, Buffett B, et al. Past and present seafloor age distributions and the temporal evolution of plate tectonic heat transport. *Earth Planet Sci Lett*, 2009, 278: 233–242
- 14 Rowley D B. Rate of plate creation and destruction: 180 Ma to present. *Geol Soc Am Bull*, 2002, 114: 927–933
- 15 Rowley D B. Extrapolating Oceanic Age Distributions: lessons from the Pacific Region. *J Geol*, 2008, 116: 587–598
- 16 Alt J C, Teagle D A H. The uptake of carbon during alteration of ocean crust. *Geochim Cosmochim Acta*, 1999, 63: 1527–1535
- 17 Foley S F, Fischer T P. An essential role for continental rifts and lithosphere in the deep carbon cycle. *Nat Geosci*, 2017, 10: 897–902
- 18 Hunt J A, Zafu A, Mather T A, et al. Spatially variable CO<sub>2</sub> degassing in the main ethiopian rift: implications for Magma storage, volatile transport, and rift-related emissions. *Geochem Geophys Geosyst*, 2017, 18: 3714–3737
- 19 Bond D P G, Wignall P B. Large igneous provinces and mass extinctions: an update. In: Keller G, Kerr A C, eds. Volcanism, Impacts, and Mass Extinctions: Causes and Effects. Geological Society of America, 2014. 29–55
- 20 Kasbohm J, Schoene B, Burgess S. Radiometric constraints on the timing, tempo, and effects of large igneous province emplacement. In: Ernst R E, Dickson A J, Bekker A, eds. Large Igneous Provinces: A Driver of Global Environmental and Biotic Changes. Geophysical Monograph Series 255. Hoboken, NJ: John Wiley & Sons, 2021. 27–82
- 21 Tian X, Buck W R. Intrusions induce global warming before continental flood basalt volcanism. *Nat Geosci*, 2022, 15: 417–422
- 22 Black B A, Karlstrom L, Mills B J W, et al. Cryptic degassing and protracted greenhouse climates after flood basalt events. *Nat Geosci*, 2024, 17: 1162–1168
- 23 Mather T A, Schmidt A. Environmental effects of volcanic volatile fluxes from subaerial large igneous provinces. In: Ernst R E, Dickson A J, Bekker A, eds. Large Igneous Provinces: A Driver of Global Environmental and Biotic Changes. Geophysical Monograph Series 255. Hoboken, NJ: John Wiley & Sons, 2021. 103–116
- 24 Lee C T A, Shen B, Slotnick B S, et al. Continental arc-island arc fluctuations, growth of crustal carbonates, and long-term climate change. *Geosphere*, 2013, 9: 21–36
- 25 McKenzie N R, Horton B K, Loomis S E, et al. Continental arc volcanism as the principal driver of icehouse-greenhouse variability. *Science*, 2016, 352: 444–447
- 26 Aiuppa A, Fischer T P, Plank T, et al. Along-arc, inter-arc and arc-to-arc variations in volcanic gas CO<sub>2</sub>/S-T ratios reveal dual source of carbon in arc volcanism. *Earth-Sci Rev*, 2017, 168: 24–47
- 27 Zhang S H, Ji W Q, Chen H B. Advances of driving mechanisms of the Early Eocene Climatic Optimum (EECO): constraints from the Linzizong volcanic rocks in southern Xizang (in Chinese). *Acta Petrol Sin*, 2022, 38: 1313–1327 [张少华, 纪伟强, 陈厚彬. 早始新世气候适宜期的驱动机制研究进展: 来自藏南林子宗火山岩的制约. 岩石学报, 2022, 38: 1313–1327]
- 28 O'Brien C L, Robinson S A, Pancost R D, et al. Cretaceous sea-surface temperature evolution: constraints from TEX<sub>86</sub> and planktonic foraminiferal oxygen isotopes. *Earth-Sci Rev*, 2017, 172: 224–247
- 29 Hasegawa H, Tada R, Jiang X, et al. Drastic shrinking of the Hadley circulation during the mid-Cretaceous Supergreenhouse. *Clim Past*, 2012, 8: 1323–1337
- 30 Foster G L, Royer D L, Lunt D J. Future climate forcing potentially without precedent in the last 420 million years. *Nat Commun*, 2017, 8: 14845
- 31 Davies A, Hunter S J, Gréselle B, et al. Evidence for seasonality in early Eocene high latitude sea-surface temperatures. *Earth Planet Sci Lett*, 2019, 519: 274–283
- 32 Rae J W B, Zhang Y G, Liu X, et al. Atmospheric CO<sub>2</sub> over the past 66 million years from marine archives. *Annu Rev Earth Planet Sci*, 2021, 49:

609–641

- 33 Hönnisch B, Royer D L, Breecker D O, et al. Toward a Cenozoic history of atmospheric CO<sub>2</sub>. *Science*, 2023, 382: eadi5177
- 34 Boucot A J, Chen X, Scotese C R. Phanerozoic Paleoclimate: An Atlas of Lithologic Indicators of Climate. Tulsa: Society for Sedimentary Geology, 2013
- 35 Suarez M B, González L A, Ludvigson G A. Quantification of a greenhouse hydrologic cycle from equatorial to polar latitudes: the mid-Cretaceous water bearer revisited. *Palaeogeogr Palaeoclimatol Palaeoecol*, 2011, 307: 301–312
- 36 Bondarenko O V, Utescher T. Early Paleogene precipitation patterns over East Asia: was there a monsoon after all? *Palaeobio Palaeoenv*, 2024, 104: 1–28
- 37 Lloyd C R. The mid-Cretaceous Earth: paleogeography, ocean circulation and temperature, atmospheric circulation. *J Geol*, 1982, 90: 393–413
- 38 Bush A B G. Numerical simulation of the cretaceous tethys circumglobal current. *Science*, 1997, 275: 807–810
- 39 Kump L R, Pollard D. Amplification of cretaceous warmth by biological cloud feedbacks. *Science*, 2008, 320: 195
- 40 Crags H J, Valdes P J, Widdowson M. Climate model predictions for the latest Cretaceous: an evaluation using climatically sensitive sediments as proxy indicators. *Palaeogeogr Palaeoclimatol Palaeoecol*, 2012, 315–316: 12–23
- 41 Kelemen P D, Steinig S, de Boer A, et al. Meridional heat transport in the DeepMIP eocene ensemble: non-CO<sub>2</sub> and CO<sub>2</sub> effects. *Paleoceanog Paleoclimatol*, 2023, 38: e2022PA004607
- 42 Kiehl J T, Shields C A, Snyder M A, et al. Greenhouse- and orbital-forced climate extremes during the early Eocene. *Phil Trans R Soc A*, 2018, 376: 20170085
- 43 Cramwinckel M J, Burls N J, Fahad A A, et al. Global and zonal-mean hydrological response to early Eocene warmth. *Paleoceanog Paleoclimatol*, 2023, 38: e2022PA004542
- 44 Farnsworth A, Lunt D J, O'Brien C L, et al. Climate sensitivity on geological timescales controlled by nonlinear feedbacks and ocean circulation. *Geophys Res Lett*, 2019, 46: 9880–9889
- 45 Inglis G N, Bragg F, Burls N J, et al. Global mean surface temperature and climate sensitivity of the early Eocene Climatic Optimum (EECO), Paleocene–Eocene Thermal Maximum (PETM), and latest Paleocene. *Clim Past*, 2020, 16: 1953–1968
- 46 Barron E J, Fawcett P J, Peterson W H, et al. A “simulation” of Mid-Cretaceous climate. *Paleoceanography*, 1995, 10: 953–962
- 47 Zhu J, Poulsen C J, Tierney J E. Simulation of Eocene extreme warmth and high climate sensitivity through cloud feedbacks. *Sci Adv*, 2019, 5: eaax1874
- 48 PALAEONSENS Project Members. Making sense of palaeoclimate sensitivity. *Nature*, 2012, 491: 683–691
- 49 Herrle J O, Schröder-Adams C J, Davis W, et al. Mid-cretaceous high arctic stratigraphy, climate, and oceanic anoxic events. *Geology*, 2015, 43: 403–406
- 50 Gale A S, Mutterlose J, Batenburg S. The Cretaceous period. In: Gradstein F M, Agterberg F P, Ogg J G, eds. *Geologic Time Scale 2020*. Amsterdam: Elsevier, 2020. 1023–1086
- 51 Zachos J C, McCarren H, Murphy B, et al. Tempo and scale of late Paleocene and early Eocene carbon isotope cycles: implications for the origin of hyperthermals. *Earth Planet Sci Lett*, 2010, 299: 242–249
- 52 Chen Z, Ding Z, Tang Z, et al. Early Eocene carbon isotope excursions: evidence from the terrestrial coal seam in the Fushun Basin, Northeast China. *Geophys Res Lett*, 2014, 41: 3559–3564
- 53 Hu X M, Li J, Han Z, et al. Two types of hyperthermal events in the Mesozoic-Cenozoic: environmental impacts, biotic effects, and driving mechanisms. *Sci China Earth Sci*, 2020, 63: 1041–1058 [胡修棉, 李娟, 韩中, 等. 中新生代两类极热事件的环境变化、生态效应与驱动机制. 中国科学: 地球科学, 2020, 50: 1023–1043]
- 54 Deines P. The carbon isotope geochemistry of mantle xenoliths. *Earth-Sci Rev*, 2002, 58: 247–278
- 55 Setty S, Cramwinckel M J, van Nes E H, et al. Loss of Earth system resilience during early Eocene transient global warming events. *Sci Adv*, 2023, 9: eade5466
- 56 Dickens G R. Rethinking the global carbon cycle with a large, dynamic and microbially mediated gas hydrate capacitor. *Earth Planet Sci Lett*, 2003, 213: 169–183
- 57 Kender S, Bogus K, Pedersen G K, et al. Paleocene/Eocene carbon feedbacks triggered by volcanic activity. *Nat Commun*, 2021, 12: 5186
- 58 Chen X, Guo H, Yao H, et al. Processes and forcing mechanisms of the carbon cycle perturbation during Cretaceous Oceanic Anoxic Event 2 (in Chinese). *Chin Sci Bull*, 2022, 67: 1677–1688 [陈曦, 郭会芳, 姚翰威, 等. 白垩纪大洋缺氧事件OAE2期间碳循环扰动的过程与机制. 科学通报, 2022, 67: 1677–1688]
- 59 Zhang F, Xiong G, Wei G Y, et al. Barium isotopes constrain the triggering mechanism of the Cretaceous OAE 2 in the Neotethys Ocean. *Earth Planet Sci Lett*, 2024, 646: 118990
- 60 Navarro-Ramirez J P, Bodin S, Heimhofer U, et al. Record of Albian to early Cenomanian environmental perturbation in the eastern sub-equatorial Pacific. *Palaeogeogr Palaeoclimatol Palaeoecol*, 2015, 423: 122–137

- 61 Bonazzi M, Bonacina G, Previde Massara E, et al. Reconstructing redox variations in a young, expanding ocean basin (Cretaceous Central Atlantic). *Cretac Res*, 2024, 153: 105681
- 62 Coccioni R, Sabatino N, Frontalini F, et al. The neglected history of Oceanic Anoxic Event 1b: insights and new data from the Poggio le Guaine section (Umbria–Marche Basin). *Stratigraphy*, 2014, 11: 245–282
- 63 Alexandre J T, Van Gilst R I, Rodríguez-lópez J P, et al. The sedimentary expression of Oceanic Anoxic Event 1b in the North Atlantic. *Sedimentology*, 2011, 58: 1217–1246
- 64 Matsumoto H, Kuroda J, Coccioni R, et al. Marine Os isotopic evidence for multiple volcanic episodes during Cretaceous Oceanic Anoxic Event 1b. *Sci Rep*, 2020, 10: 12601
- 65 Sabatino N, Ferraro S, Coccioni R, et al. Mercury anomalies in upper Aptian-lower Albian sediments from the Tethys realm. *Palaeogeogr Palaeoclimatol Palaeoecol*, 2018, 495: 163–170
- 66 Zhao X, Zheng D, Wang H, et al. Carbon cycle perturbation and mercury anomalies in terrestrial Oceanic Anoxic Event 1b from Jiuquan Basin, NW China. In: Chang S C, Zheng D, eds. Mesozoic Biological Events and Ecosystems in East Asia. London: Geological Society, London, 2022. 185–196
- 67 Bottini C, Erba E. Mid-Cretaceous paleoenvironmental changes in the western Tethys. *Clim Past*, 2018, 14: 1147–1163
- 68 Li M, Bralower T J, Kump L R, et al. Astrochronology of the Paleocene-Eocene Thermal Maximum on the Atlantic coastal plain. *Nat Commun*, 2022, 13: 5618
- 69 Kent D V, Cramer B S, Lanci L, et al. A case for a comet impact trigger for the Paleocene/Eocene thermal maximum and carbon isotope excursion. *Earth Planet Sci Lett*, 2003, 211: 13–26
- 70 Higgins J A, Schrag D P. Beyond methane: towards a theory for the Paleocene–Eocene Thermal Maximum. *Earth Planet Sci Lett*, 2006, 245: 523–537
- 71 Frieling J, Peterse F, Lunt D J, et al. Widespread warming before and elevated barium burial during the Paleocene–Eocene thermal maximum: evidence for methane hydrate release? *Paleoceanogr Palaeoclimatol*, 2019, 34: 546–566
- 72 Schlanger S O, Jenkyns H C. Cretaceous oceanic anoxic events: causes and consequences. *Neth J Geosci*, 1976, 55: 179–184
- 73 Erba E, Bottini C, Weisert H J, et al. Calcareous nannoplankton response to surface-water acidification around oceanic anoxic event 1a. *Science*, 2010, 329: 428–432
- 74 Gingerich P D. Environment and evolution through the Paleocene–Eocene thermal maximum. *Trends Ecol Evol*, 2006, 21: 246–253
- 75 Heimhofer U, Wucherpfennig N, Adatte T, et al. Vegetation response to exceptional global warmth during Oceanic Anoxic Event 2. *Nat Commun*, 2018, 9: 3832
- 76 Carmichael M J, Inglis G N, Badger M P S, et al. Hydrological and associated biogeochemical consequences of rapid global warming during the Paleocene-Eocene Thermal Maximum. *Glob Planet Change*, 2017, 157: 114–138
- 77 Keller C E, Hochuli P A, Weissert H, et al. A volcanically induced climate warming and floral change preceded the onset of OAE1a (Early Cretaceous). *Palaeogeogr Palaeoclimatol Palaeoecol*, 2011, 305: 43–49
- 78 Zhang X, Li S, Wang X, et al. Expression of the early Aptian Oceanic Anoxic Event (OAE) 1a in lacustrine depositional systems of East China. *Glob Planet Change*, 2021, 196: 103370
- 79 Fan D, Shan X, Makeen Y M, et al. Response of a continental fault basin to the global OAE1a during the Aptian: hongmiaozi Basin, Northeast China. *Sci Rep*, 2021, 11: 7229
- 80 Xu X T, Shao L Y, Eriksson K A, et al. Terrestrial records of the early Albian Ocean Anoxic Event: evidence from the Fuxin lacustrine basin, NE China. *Geosci Front*, 2022, 13: 101275
- 81 Chen H, Xu Z, Bayon G, et al. Enhanced hydrological cycle during Oceanic Anoxic Event 2 at southern high latitudes: new insights from IODP Site U1516. *Glob Planet Change*, 2022, 209: 103735
- 82 Pagani M, Pedentchouk N, Huber M, et al. Arctic hydrology during global warming at the Palaeocene/Eocene thermal maximum. *Nature*, 2006, 442: 671–675
- 83 Kender S, Stephenson M H, Riding J B, et al. Marine and terrestrial environmental changes in NW Europe preceding carbon release at the Paleocene–Eocene transition. *Earth Planet Sci Lett*, 2012, 353–354: 108–120
- 84 Chen Z, Dong X, Wang X, et al. Spatial change of precipitation in response to the Paleocene-Eocene thermal Maximum warming in China. *Glob Planet Change*, 2020, 194: 103313
- 85 Pujalte V, Schmitz B, Payros A. A rapid sedimentary response to the Paleocene-Eocene Thermal Maximum hydrological change: new data from alluvial units of the Tremp-Graus Basin (Spanish Pyrenees). *Palaeogeogr Palaeoclimatol Palaeoecol*, 2022, 589: 110818
- 86 Kraus M J, Riggins S. Transient drying during the Paleocene–Eocene Thermal Maximum (PETM): analysis of paleosols in the bighorn basin, Wyoming. *Palaeogeogr Palaeoclimatol Palaeoecol*, 2007, 245: 444–461
- 87 Chen Z, Li C, Yang S, et al. Two sites in east Asia add to spatiotemporal heterogeneity of wildfire activity across the Paleocene–Eocene Thermal

- Maximum. *Geophys Res Lett*, 2025, 52: e2024GL113829
- 88 Urban M C. Accelerating extinction risk from climate change. *Science*, 2015, 348: 571–573
- 89 Carvalho M R, Jaramillo C, de la Parra F, et al. Extinction at the end-Cretaceous and the origin of modern Neotropical rainforests. *Science*, 2021, 372: 63–68
- 90 Bansal M, Morley R J, Nagaraju S K, et al. Southeast Asian Dipterocarp origin and diversification driven by Africa-India floristic interchange. *Science*, 2022, 375: 455–460
- 91 Duperon-Laudoueneix M. Découverte d'un tronc de palmier dans les dépôts détritiques paléogènes du sud de la Charente (Sud-Ouest de la France). *Trav Lab Géogr Phys Appl*, 1984, 8: 59–69
- 92 Srivastava R, Srivastava G, Dilcher D L, et al. Coryphoid palm leaf fossils from the Maastrichtian–Danian of central India with remarks on phytogeography of the Coryphoideae (Arecaceae). *PLoS One*, 2014, 9: e111738
- 93 Suan G, Popescu S M, Suc J P, et al. Subtropical climate conditions and mangrove growth in Arctic Siberia during the early Eocene. *Geology*, 2017, 45: 539–542
- 94 Zhou Z K, Wang N, Liu J, et al. The discovery of the Eocene genus *Palibinia* from Xizang, China and its geological and biological significances (in Chinese). *Quat Sci*, 2024, 44: 1469–1481 [周浙昆, 王楠, 刘佳, 等. 西藏始新世狭叶梅属(*Palibinia*)的发现及其地质学和生物学意义. 第四纪研究, 2024, 44: 1469–1481]
- 95 Jaramillo C, Ochoa D, Contreras L, et al. Effects of rapid global warming at the Paleocene-Eocene boundary on neotropical vegetation. *Science*, 2010, 330: 957–961
- 96 Wing S L, Harrington G J, Smith F A, et al. Transient floral change and rapid global warming at the Paleocene-Eocene boundary. *Science*, 2005, 310: 993–996
- 97 Asar Y, Ho S Y W, Sauquet H. Early diversifications of angiosperms and their insect pollinators: were they unlinked? *Trends Plant Sci*, 2022, 27: 858–869
- 98 Labandeira C C, Johnson K R, Wilf P. Impact of the terminal Cretaceous event on plant-insect associations. *Proc Natl Acad Sci USA*, 2002, 99: 2061–2066
- 99 Wilf P, Labandeira C C, Kress W J, et al. Timing the radiations of leaf beetles: spines on gingers from Latest Cretaceous to recent. *Science*, 2000, 289: 291–294
- 100 Carvalho M R, Wilf P, Barrios H, et al. Insect leaf-chewing damage tracks herbivore richness in modern and ancient Forests. *PLoS One*, 2014, 9: e94950
- 101 Bown P R, Lees J A, Young J R. Calcareous nannoplankton evolution and diversity through time. In: Thierstein H R, Young J R, eds. *Coccolithophores*. Berlin and Heidelberg: Springer, 2004. 481–508
- 102 Kiessling W. Radiolarian diversity patterns in the latest Jurassic–earliest Cretaceous. *Palaeogeogr Palaeoclimatol Palaeoecol*, 2002, 187: 179–206
- 103 Caves J K, Jost A B, Lau K V, et al. Cenozoic carbon cycle imbalances and a variable weathering feedback. *Earth Planet Sci Lett*, 2016, 450: 152–163
- 104 Galy V, France-Lanord C, Beyssac O, et al. Efficient organic carbon burial in the Bengal fan sustained by the Himalayan erosional system. *Nature*, 2007, 450: 407–410
- 105 Foreman B Z, Heller P L, Clementz M T. Fluvial response to abrupt global warming at the Palaeocene/Eocene boundary. *Nature*, 2012, 491: 92–95
- 106 Pogge von Strandmann P A E, Jenkyns H C, Woodfine R G. Lithium isotope evidence for enhanced weathering during Oceanic Anoxic Event 2. *Nat Geosci*, 2013, 6: 668–672
- 107 Chen Z, Ding Z, Yang S, et al. Strong coupling between carbon cycle, climate, and weathering during the Paleocene-Eocene Thermal Maximum. *Geophys Res Lett*, 2023, 50: e2023GL102897
- 108 Chenot E, Deconinck J F, Pucéat E, et al. Continental weathering as a driver of Late Cretaceous cooling: new insights from clay mineralogy of Campanian sediments from the southern Tethyan margin to the Boreal realm. *Glob Planet Change*, 2018, 162: 292–312
- 109 Farnsworth A, Lunt D J, Robinson S A, et al. Past East Asian monsoon evolution controlled by paleogeography, not CO<sub>2</sub>. *Sci Adv*, 2019, 5: eaax1697
- 110 Wang C, Scott R W, Wan X, et al. Late Cretaceous climate changes recorded in Eastern Asian lacustrine deposits and North American Epieric sea strata. *Earth-Sci Rev*, 2013, 126: 275–299
- 111 Guo H, Chen X, Yao H, et al. Quantifying the pattern of organic carbon burial through Cretaceous Oceanic Anoxic Event 2. *Earth-Sci Rev*, 2024, 257: 104903
- 112 Watson A J, Lenton T M, Mills B J W. Ocean deoxygenation, the global phosphorus cycle and the possibility of human-caused large-scale ocean anoxia. *Phil Trans R Soc A*, 2017, 375: 20160318
- 113 Guo L, Xiong S, Mills B J W, et al. Acceleration of phosphorus weathering under warm climates. *Sci Adv*, 2024, 10: eadm7773

- 114 Reershemius T, Planavsky N J. What controls the duration and intensity of ocean anoxic events in the Paleozoic and the Mesozoic? *Earth-Sci Rev*, 2021, 221: 103787
- 115 Jenkyns H C. Geochemistry of oceanic anoxic events. *Geochem Geophys Geosyst*, 2010, 11: q03004
- 116 Martin J H, Fitzwater S E. Iron deficiency limits phytoplankton growth in the north-east Pacific subarctic. *Nature*, 1988, 331: 341–343
- 117 Li G, Elderfield H. Evolution of carbon cycle over the past 100 million years. *Geochim Cosmochim Acta*, 2013, 103: 11–25
- 118 Berner R A. The long-term carbon cycle, fossil fuels and atmospheric composition. *Nature*, 2003, 426: 323–326
- 119 Owens J D, Lyons T W, Lowery C M. Quantifying the missing sink for global organic carbon burial during a Cretaceous oceanic anoxic event. *Earth Planet Sci Lett*, 2018, 499: 83–94
- 120 Jiang H, Lee C T A. On the role of chemical weathering of continental arcs in long-term climate regulation: a case study of the Peninsular Ranges batholith, California (USA). *Earth Planet Sci Lett*, 2019, 525: 115733

Summary for “白垩纪–古近纪热室地球”

## Hothouse Earth during the Cretaceous–Paleogene period: an overview

Shiling Yang<sup>1,2\*</sup>, Lin Chen<sup>1,2</sup>, Weiqiang Ji<sup>1</sup>, Tao Su<sup>3</sup>, Shijun Jiang<sup>4</sup>, Zuoling Chen<sup>1</sup>, Xiaofang Huang<sup>1</sup>, Licheng Guo<sup>1</sup>, Yongda Wang<sup>5</sup>, Hehe Jiang<sup>1</sup>, Dangpeng Xi<sup>6</sup>, Zihua Tang<sup>1</sup>, Shihao Zhang<sup>1</sup>, Minmin Sun<sup>1</sup> & Fuyuan Wu<sup>1,2</sup>

<sup>1</sup> State Key Laboratory of Lithospheric and Environmental Coevolution, Institute of Geology and Geophysics, Chinese Academy of Sciences, Beijing 100029, China

<sup>2</sup> College of Earth and Planetary Sciences, University of Chinese Academy of Sciences, Beijing 100049, China

<sup>3</sup> Institute of Sedimentary Geology, Chengdu University of Technology, Chengdu 610059, China

<sup>4</sup> State Key Laboratory of Marine Resource Utilization in South China Sea, Hainan University, Haikou 570228, China

<sup>5</sup> School of Water Conservancy and Environment, University of Jinan, Jinan 250022, China

<sup>6</sup> State Key Laboratory of Geomicrobiology and Environmental Changes, China University of Geosciences, Beijing 100083, China

\* Corresponding author, E-mail: [yangsl@mail.igcas.ac.cn](mailto:yangsl@mail.igcas.ac.cn)

As anthropogenic carbon emissions continue to rise, global temperatures are experiencing unprecedented increases. In response to the looming threats of climate change, the Paris Agreement proposed the goal of limiting global warming to 1.5–2.0°C and advocated for global emission reductions. However, recent studies suggest that even if these targets are met, internal feedback mechanisms within the climate system could still propel global warming beyond critical thresholds, potentially shifting Earth's climate from cyclical glacial-interglacial alternation to a hothouse state. Notably, 2024 was the hottest year on record, with the global average surface temperature 1.55°C higher than pre-industrial levels, making it the first calendar year since the Industrial Revolution to exceed 1.5°C of warming. If the current warming trend observed in recent decades continues, the Earth's average temperature could reach 20°C by ~2300, resulting in a permanent hothouse state. This alarming prospect raises concerns within both the scientific community and the general public about the potential for catastrophic outcomes.

The Cretaceous–Paleogene period represents Earth's most recent prolonged hothouse state, characterized by sustained high temperatures and elevated atmospheric CO<sub>2</sub> concentrations. Understanding this period offers critical insights into future climate scenarios. This study synthesizes current knowledge of the Cretaceous–Paleogene hothouse Earth, exploring its driving mechanisms, environmental characteristics, ecological responses, and ultimate termination. Key findings include: (1) through integrated analysis of carbon emission patterns from mid-ocean ridges, continental rifts, large igneous provinces, and continental arcs, coupled with paleoclimatic records, we propose that continental arc magmatism was likely the primary driver of the Cretaceous–Paleogene hothouse conditions. (2) Multiple episodes of carbon cycle perturbations, lasting 10<sup>4</sup>–10<sup>5</sup> years, characterized the hothouse climate regime, driving rapid climatic warming events. These include the Cretaceous Oceanic Anoxic Events (OAEs) and the Paleogene hyperthermal events (e.g., the Paleocene–Eocene Thermal Maximum (PETM)). The OAEs are characterized by extensive black shale deposition, with distinct positive carbon isotope excursions observed during OAE1a, OAE1d, and OAE2, while OAE1b is marked by a notable negative excursion. In contrast, the Paleogene hyperthermal events consistently exhibit negative carbon isotope excursions with limited black shale deposition. This pronounced dichotomy in geochemical signatures and depositional patterns between these events can be primarily explained by fundamental differences in both the nature of carbon sources and the underlying perturbation mechanisms. (3) Hyperthermal events, characterized by pronounced negative carbon isotope excursions, occurred during prolonged periods of warming, indicating increased vulnerability of Earth's surface organic carbon reservoirs to increases in global temperature. OAE1b, PETM, and subsequent Eocene hyperthermal events were likely triggered by perturbations in these reservoirs, highlighting the necessity for comparative studies on their respective carbon emission fluxes and associated environmental impacts. (4) The hyperthermal events were associated with intensified hydrological cycles, characterized by enhanced high-latitude precipitation and complex spatial variability in mid- to low-latitude rainfall patterns. (5) The hothouse climate facilitated the expansion and diversification of thermophilic plant groups, promoting the spread of forest from low to middle and high latitudes and enhancing terrestrial plant diversity. In marine environments, there was also an increase in the diversity of dinoflagellate cysts, calcareous nannofossils, and planktic foraminifera.

This synthesis highlights that the Cretaceous–Paleogene hothouse state was fundamentally maintained by deep Earth carbon emissions, while its termination was governed by carbon sequestration through enhanced chemical weathering and organic matter burial. However, significant uncertainties remain regarding quantitative carbon fluxes, spatial patterns of hydrological changes, and ecosystem responses to rapid warming. Future research directions should emphasize integrated Earth system approaches to better constrain these critical aspects of hothouse Earth dynamics.

**Cretaceous–Paleogene, hothouse Earth, deep Earth process, carbon cycle, hyperthermal event, environmental change**

doi: [10.1360/CSB-2025-0278](https://doi.org/10.1360/CSB-2025-0278)